Experimental verification of Lorentz' linearization procedure for quadratic friction

Terra, G.M.; van den Berg, W.J.; Maas, L.R.M.

DOI
10.1016/j.fluiddyn.2005.01.005
Publication date
2005

Published in
Fluid Dynamics Research

Available online at www.sciencedirect.com
SCIENCE DIRECT®
Fluid Dynamics Research 36 (2005) 175–188
FLUID DYNAMICS RESEARCH

Experimental verification of Lorentz' linearization procedure for quadratic friction

Guido M. Terra[a, b, *], Willem Jan van de Berg[a, c], Leo R.M. Maas[a]

[a] *Physics Department, Royal Netherlands Institute for Sea Research, P.O. Box 59, NL-1790 AB Den Burg, The Netherlands*
[b] *Korteweg-de Vries Institute for Mathematics, University of Amsterdam, Plantage Muidergracht 24, NL-1018 TV Amsterdam, The Netherlands*
[c] *Institute for Marine and Atmospheric research Utrecht, P.O. Box 80000, NL-3508 TA Utrecht, The Netherlands*

Received 14 October 2004; received in revised form 18 January 2005; accepted 25 January 2005

Communicated by A.D. Gilbert

Abstract

We present results from laboratory experiments in a 'tidal tank', demonstrating the resonant response of the Helmholtz mode in an almost-enclosed basin. In particular the dependence of the response curve (amplification of the tide in the basin relative to the tidal signal at sea as a function of forcing frequency) on the tidal amplitude due to the nonlinear influence of dissipation is observed. Although Lorentz' linearization procedure for coping with this nonlinear effect was already developed at the beginning of the previous century, quantitative experimental validation in this context has not yet been provided. The experimental results presented in this paper show good agreement with theory.

PACS: 92.10.Hm; 92.10.Jn; 92.10.Sx

Keywords: Wave amplification; Harbor resonance; Quadratic friction; Head loss; Flow separation; Oscillatory flow; Lorentz'/equivalent linearization; Laboratory tests

* Corresponding author. Physics Department, Royal Netherlands Institute for Sea Research, P.O. Box 59, NL-1790 AB Den Burg, The Netherlands.
E-mail address: terra@nioz.nl (G.M. Terra).

0169-5983/$30.00 © 2005 Published by The Japan Society of Fluid Mechanics and Elsevier B.V.

doi:10.1016/j.fluiddyn.2005.01.005

1. Introduction

Tidal motion is a key feature in many coastal areas, with tidal ranges of 1–3 m (Dutch Wadden Sea) up to 16 m (Bay of Fundy). At those locations, it by far exceeds the *equilibrium tide* which represents direct gravitational forcing (if the Earth were completely covered by water, neglecting inertia) by the moon (54 cm) and the sun (26 cm). The amplification is a result of resonance when the directly driven ocean tide propagates into co-oscillating coastal seas. Linear theory describing this is well established and is reviewed in e.g. Defant (1961).

Resonance occurs if the tidal period is close to one of the eigenmodes of the basin, such as the *quarter wavelength* modes in half open channel-like basins, or the *Helmholtz* or *pumping mode* in almost-enclosed basins. The latter is a relatively simple mode characterized by uniform sealevel elevation within basins that are small compared to the tidal wavelength and co-oscillate with an adjacent sea/ocean through a narrow inlet. The balance between the inertia of the flow through the inlet and the restoring force due to the sealevel difference between that at sea and in the basin determines the oscillation (Miles, 1974).

Dissipation of energy in resonant Helmholtz basins, which is the main interest in this paper, is through radiation damping, bottom friction and *head loss* (pressure drop) due to flow separation. Radiation damping is adequately described linearly but leads to the so-called harbor paradox (Carrier et al., 1971; Miles, 1974): intuitively one would expect suppression of the response to external forcing when decreasing the width of the inlet, due to increased screening. However, the maximum and mean square response appear to increase, because radiation of energy is reduced. By including the effect of *head loss* due to flow separation at the inlet this paradox is resolved by e.g. Mei et al. (1974). Using hydraulic theory they show that the head loss term depends quadratically on the fluid velocity. Actually this is the same form as Chezy's law, commonly used to model bottom friction.

In order to evaluate the influence of the quadratic (bottom) friction term Lorentz (1922, 1926) proposed to replace it by a linear term with the friction coefficient chosen such that the energy dissipation per tidal cycle would be the same as when the nonlinear law were used. Mei (1989) mentions Lorentz' linearization method under the name of *equivalent linearization*. A number of different approaches can be found in the literature as well, including asymptotic expansions of the quadratic friction term (e.g. Kabbaj and Le Provost, 1980). All of those methods are virtually equivalent, at least to first order. Hence the simplest approach of Zimmerman (1992) is followed in this paper.

The calculations of Lorentz (1926) have been confirmed quite well by field observations in the Dutch Wadden Sea (Thijsse, 1972). Nonlinear aspects express themselves in the generation of higher harmonics distorting the tidal curve to become asymmetric (Aubrey and Speer, 1985, and references therein). Laboratory experiments have been performed as well, but have mainly focused on validating linear theory (e.g. McNown, 1952; Lee, 1971) or on the distortion of the tidal curve (Lepelletier and Raichlen, 1987). Experiments to corroborate Lorentz' linearization theory, by comparing the response curves at different forcing amplitudes, seem to be missing. Although Horikawa and Nishimura (1970) do present results for different amplitudes, they rate them as less accurate owing to the deformation of the waves and do not provide an adequate quantitative comparison with theory. Both Bowers (1977) and De Girolamo (1996) state qualitatively that the head loss effect is found to cause the amplification factor to decrease with increasing amplitude in their preliminary experiments. However, their main focus is on the generation of harbor oscillations due to the nonlinear setup/setdown by wave groups. Although they do mention the quadratic dependence of the energy loss on velocity, no quantitative analysis is given by them either. In particular, no reference to Lorentz' linearization principle is made. Equivalent linearization is mentioned

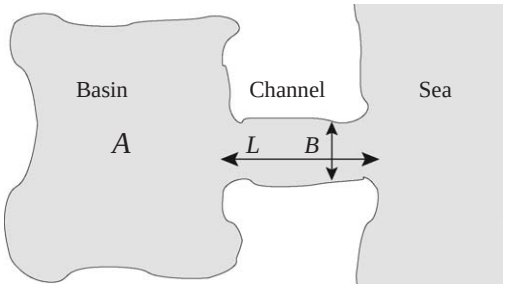

Fig. 1. Top view sketch of an almost-enclosed tidal basin with horizontal area A, co-oscillating with the tide at sea through an inlet channel of width B, length L and depth H.

by Martinez and Naverac (1988). They provide good quality experimental data, but their focus is on the effect of changing the entrance width to their basins. Their analysis of the data is based on insufficiently developed theory neglecting inertia. As a consequence the dependence on forcing amplitude is not captured well and they conclude that the coefficient in the nonlinear friction law strongly depends on the forcing amplitude.

In order to fill the lack of experimental validation of Lorentz' linearization principle, we present a quantitative comparison between our measurements and the results of a simple model for the Helmholtz mode with Lorentz' linearized friction, which does predict the dependence of the response curves on the forcing amplitude. After a brief overview of the theory in Section 2 and a description of the experimental setup in Section 3, the results are discussed in Section 4. The paper is concluded with an estimation of the domain of validity of Lorentz' linearization theory using a renormalization method and numerical integration and a discussion of the relevance in the geophysical context.

2. Theory

Consider an almost-enclosed basin with horizontal area A connected to the sea by a channel of length L, width B and depth H, as shown in Fig. 1, which is forced by a tidal signal at sea with angular frequency ω. Its dimensions are assumed to be much smaller than the tidal wavelength $\lambda = 2\pi\sqrt{gH}/\omega$, such that the tidal wave traverses the basin "instantaneously". Hence the water level in the basin can be described by a single value ζ, the elevation relative to the still water level. Water flows into the basin through the channel with velocity u. All dynamics are concentrated in the channel, where the elevation difference between sea and basin drives the flow, balanced by the inertia of the water in the channel and bottom friction/head loss. Actually, the channel length L in (1a) measures the inertia of the system. The (relatively small) contribution of flow outside the channel causes the effective length L_{eff}, which determines the eigenfrequency ω_0 defined below, to be slightly longer than the physical length of the channel, the "added mass effect". From here on each occurrence of L relates to effective length, the notation L_{eff} is used only if confusion with physical length might occur. Bottom friction is commonly described by Chezy's law $(c_{\mathrm{D}}/H)\,|u|u$, with drag coefficient $c_{\mathrm{D}} \approx 0.0025$ determined empirically (Parker, 1991). The head loss due to flow separation is parameterized by $(f/L)\,|u|u$ and differs only in the formulation of the coefficient; f has to be determined empirically as well. Indeed, based on computer simulations, Ito (1970) reports that the harbor paradox is resolved by including this term and the vulnerability of the Port of Ofunato

to tsunamis decreased considerably due to the partial closure of the entrance by a breakwater. He found that $f \approx 1.5$ gave the best results when comparing the numerical simulations with observations from tide gauges. The dynamics of the system can be described by the equations for momentum and mass conservation:

$$\frac{\mathrm{d}u}{\mathrm{d}t} = \frac{g}{L}(\zeta_\mathrm{e} - \zeta) - \frac{\tilde{f}}{L}|u|u, \tag{1a}$$

$$A\,\frac{\mathrm{d}\zeta}{\mathrm{d}t} = Ou, \tag{1b}$$

where $\zeta_\mathrm{e} = \alpha_\mathrm{e}\cos(\omega t) = \mathrm{Re}[\alpha_\mathrm{e}\,\mathrm{e}^{\mathrm{i}\omega t}]$ is the prescribed elevation at sea and $O = BH$ is the channel cross-section. The head loss coefficient $\tilde{f}/L$ is considered to include bottom friction as well ($\tilde{f}/L = f/L + c_\mathrm{D}/H$). Note that radiation damping is not modeled here explicitly but is assumed to be already incorporated in ζ_e, i.e. ζ_e is considered to be the tidal signal at the seaward entrance *with the basin present*. In analyzing the experimental results we will also compare the measurements inside the basin with the forcing signal at sea as it is measured simultaneously.

The Lorentz' linearization principle amounts to replacing the nonlinear head loss term $(\tilde{f}/L)\,|u|u$ by ru, with effective linear friction coefficient r to be determined. In that case system (1) is linear and the response will be of the form $\zeta = |\alpha|\cos(\omega t + \varphi) = \mathrm{Re}[\alpha\,\mathrm{e}^{\mathrm{i}\omega t}]$, where $\alpha = |\alpha|\mathrm{e}^{\mathrm{i}\varphi}$, and consequently $u = -(A/O)\omega|\alpha|\sin(\omega t + \varphi)$. Lorentz' energy principle states that the energy dissipation per tidal cycle should be the same for both formulae: $\langle ru^2\rangle = \langle(\tilde{f}/L)|u|u^2\rangle$, in which $\langle\cdot\rangle$ denotes averaging over a tidal cycle. Evaluation of the corresponding integrals leads to $r = v_0\omega|\alpha|$, with $v_0 = (8/3\pi)(\tilde{f}A/OL)$, i.e. effective friction increases linearly with tidal amplitude in the basin. Using the linear expression for friction, (1) can be simplified to

$$\frac{\mathrm{d}^2\zeta}{\mathrm{d}t^2} = \omega_0^2\,(\zeta_\mathrm{e} - \zeta) - v_0\omega|\alpha|\frac{\mathrm{d}\zeta}{\mathrm{d}t},$$

in which $\omega_0^2 = gO/(AL)$ is the eigenfrequency of the Helmholtz mode. Substituting $\zeta = \mathrm{Re}[\alpha\,\mathrm{e}^{\mathrm{i}\omega t}]$ the complex response equation is found:

$$(\omega_0^2 - \omega^2)\alpha + \mathrm{i}v_0\omega^2|\alpha|\alpha = \omega_0^2\alpha_\mathrm{e}. \tag{2}$$

By taking the square modulus of this equation it is possible to solve for $|\alpha|$ and find

$$\frac{|\alpha|}{|\alpha_\mathrm{e}|} = \sqrt{\frac{\sqrt{(1-(\omega/\omega_0)^2)^4 + 4v_0^2(\omega/\omega_0)^4|\alpha_\mathrm{e}|^2} - (1-(\omega/\omega_0)^2)^2}{2v_0^2(\omega/\omega_0)^4|\alpha_\mathrm{e}|^2}}, \tag{3}$$

which can be combined with (2) to find the phase lag $\varphi \in (-\pi, 0)$ as well, from $\varphi = \arccos((1 - (\omega/\omega_0)^2)\,(|\alpha|/\alpha_\mathrm{e}))$. Differentiating the square modulus of (2) with respect to ω, equating the derivative of $|\alpha|$ to zero and using the result to eliminate either ω or α_e, one can maximize (3) with respect to ω. As

a function of forcing amplitude α_e maximum amplification is given by

$$\frac{|\alpha|_{\max}}{\alpha_e} = \sqrt{\frac{1}{2} + \frac{1}{2}\sqrt{1 + \frac{4}{\nu_0^2 \alpha_e^2}}}. \tag{4}$$

As a function of ω one has $|\alpha|_{\max}/\alpha_e = (1 - (\omega/\omega_0)^2)^{-1/2}$, which will be indicated by a dotted line in the response diagram (Fig. 4(a)).

3. Experimental setup

A sketch of the experimental setup is shown in Fig. 2. The area of interest is the "basin" of 0.916 m^2. Instead of a channel, a completely submerged pipe is used to connect the basin to the forcing tide at "sea". In this way, the cross-section O does not depend on the water-level elevation ζ, which would otherwise introduce (additional) nonlinear effects (Miles, 1981). The experiments presented in this paper were performed using a circular pipe with a length of 441 mm and 76.4 mm diameter. Without the "added mass effect" increasing the effective pipe length, the Helmholtz frequency is expected to be $\omega_0 = 0.33\,\mathrm{rad\,s^{-1}} = 53 \times 10^{-3}\,\mathrm{Hz}$ (18.8 s period). The water depth at rest was set to be about 15 cm above the bottom of the basin and was checked not to influence the measurements as long as the pipe remains completely submerged. A forcing tank is immersed in the water and is lifted and lowered by a properly counterbalanced servomotor. The control signal can be generated by the computer. In principle the forcing signal may consist of many frequency components, but harmonic forcing only is considered in this paper. The water expelled by the forcing tank, moves through the conduit underneath the basin area towards the sea. A grating was inserted in order to help the water level rise at sea to be uniform, but it did not prevent the occurrence of a standing wave: depending on the forcing frequency amplitudes are higher at the far end of the sea. The amplitude of the control signal is adjusted to obtain the desired forcing amplitude at the mouth of the basin (cf. the discussion at the end of this section), so this has no influence on the measurements. Acoustic sensors are used for nonintrusive measurements of water-level elevation. They are located above the tank and emit an acoustic signal at 300 kHz down to the water surface and measure the return time of the reflected signal, like an echo sounder. Their resolution is 0.36 mm, the

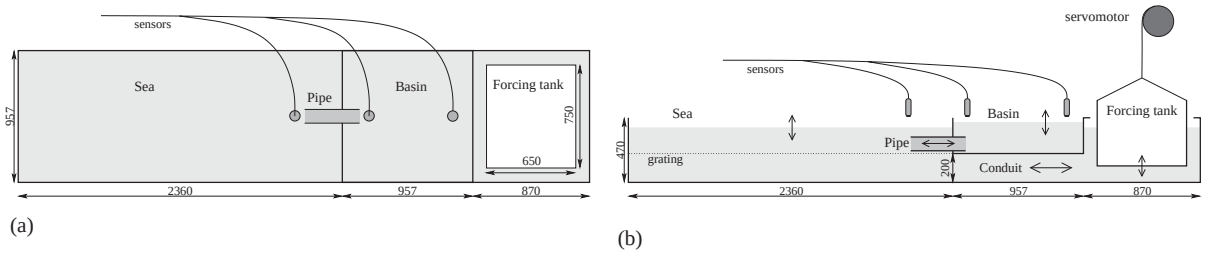

Fig. 2. Sketch of the experimental setup, dimensions in mm are indicated. The forcing tank is set into motion by a servomotor. The water expelled by the tank moves through the conduit underneath the basin area to the "sea". The tidal signal thus generated at sea, propagates into the basin through a completely submerged pipe. The water-level elevation is measured by acoustic sensors at the indicated positions. Because the tide in the basin is nearly uniform, the measurements for the sensors in the basin are virtually the same. (a) Top view, (b) side view.

standard deviation of the noise is similar. Significant outliers of some centimeters occur and are dismissed from the analysis.

No dissipators have been installed at the sidewalls of the sea. Raichlen and Ippen (1965) warn that consequent reflections have a dramatic effect on the response curves. They define the amplification factor as the ratio of the tidal response amplitude in the basin over the amplitude at the seaward entrance *if the basin were closed*, i.e. not present. Indeed, radiation damping effects changing the actual tidal forcing signal at the seaward entrance, are quite different in a finite reflective sea than in a semi-infinite reflectionless sea. We however choose to correct the motion of the forcing tank such that the amplitude at the seaward entrance is the same for all frequencies and define the amplification factor as the ratio of the response amplitude in the basin over the amplitude at sea *with the basin connected to it*, as it is measured simultaneously. This effectively boils down to eliminating the effect of radiation damping and circumvents the problems mentioned by Raichlen and Ippen (1965).

4. Results

A sample time series from our measurements is shown in Fig. 3. This measurement was performed at a forcing frequency $\omega = 0.0420$ Hz $= 0.264\,\mathrm{rad\,s^{-1}}$ and forcing amplitude α_e approximately 2 mm. Measurements at the seaward pipe entrance are indicated by dots. Pluses and crosses are used for the

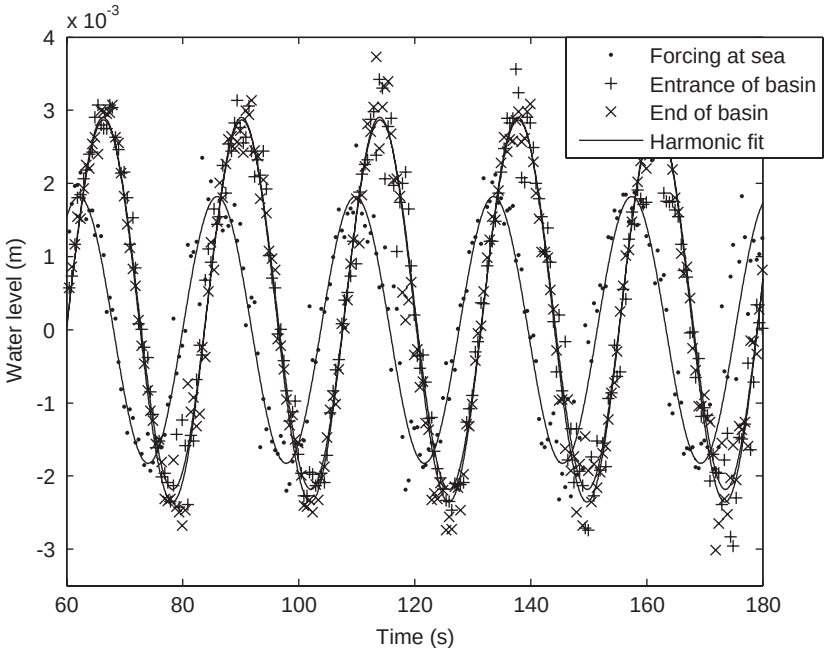

Fig. 3. Sample time series of measurements at forcing frequency 0.0420 Hz and forcing amplitude approximately 2 mm. Dots indicate measurements from the sensor at sea, pluses and crosses indicate measurements at the entrance and end of the basin, respectively. Solid curves show harmonic fits to the respective time series. The two curves inside the basin are nearly indistinguishable, consistent with a Helmholtz mode of uniform basin tide.

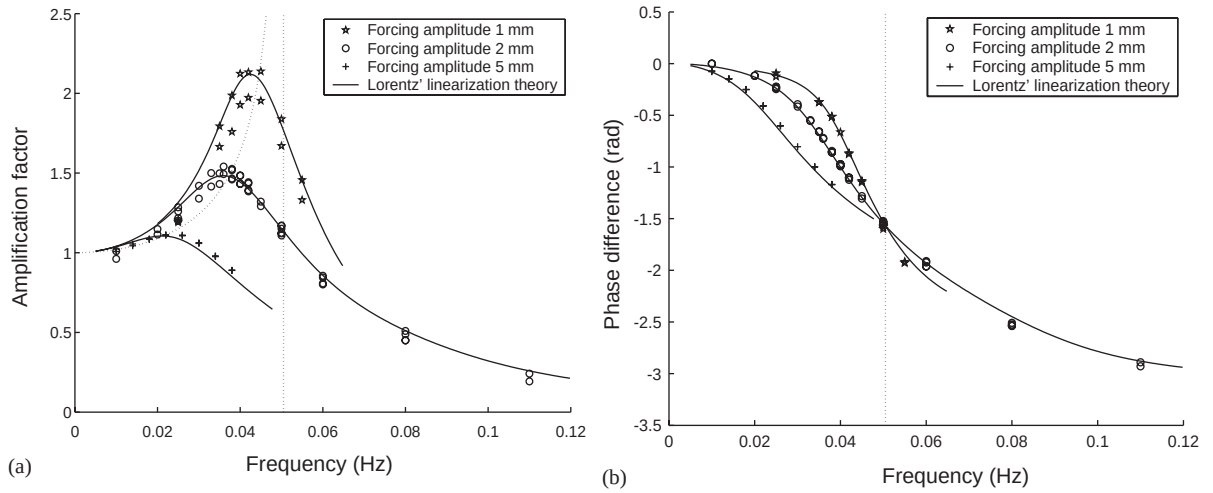

Fig. 4. Response curves: (a) amplification factor $|\alpha|/\alpha_e$ and (b) phase lag ϕ between the tide at sea and in the basin as a function of forcing frequency $\omega/(2\pi)$. Three series of measurements with forcing amplitudes $\alpha_e \approx 1, 2, 5$ mm are shown, for each of which results for two sensors in the basin have been obtained. Slight amplitude differences between both basin sensors can be noted, in particular at 1 mm forcing amplitude. Solid curves show the fit to theory (3). The Helmholtz frequency $\omega_0 = 0.0505$ Hz is indicated by a dotted vertical line, a dotted curve connects the maxima according to (4). Note that one fit is used to describe all three curves. Apparently the decrease of the resonator's quality is adequately described by Lorentz' linearization theory.

measurements in the basin. Amplification and phase lag between the tide at sea and in the basin are clearly visible. Note that the signals of both sensors inside the basin are virtually the same, so the assumption of uniform tide in the basin is satisfied indeed. Harmonic analysis has been used to fit the measurements to a sum of sinusoids at the forcing frequency and significant overtides, if any. In most cases, no significant overtides were found. Only for particular frequencies, if one of the overtides was resonant with the eigenfrequency ~ 0.45 Hz of the entire system (sea and forcing tank), secondary oscillations were found at sea. They appeared not to extend into the basin though and there are no indications of their influence on the response curves for the main component. The harmonic fits are shown in Fig. 3 as well.

From the amplitudes found this way, the amplification factor and phase lag of the forcing frequency component are calculated. By plotting them as a function of forcing frequency, the response curves are determined, see Fig. 4, for three different forcing amplitudes $\alpha_e \approx 1, 2, 5$ mm. The theory according to (2) has been fitted to the measurements minimizing the least square error in the complex α/α_e plane. Because the effective length differs from the actual pipe length due to the added mass effect it has to be determined empirically. The same holds good for the head loss parameter $\tilde{f}$. Therefore, ω_0 and v_0 are used as fitting parameters. The curves shown in Fig. 4 are for the best fit with $\omega_0 = 50.5 \pm 0.9 \times 10^{-3}$ Hz $= 0.317 \pm 0.006$ rad s^{-1}, $v_0 = 374 \pm 9$ m^{-1}. So the effective pipe length $L_{\text{eff}} = 48.9 \pm 1.7$ cm is 4.8 cm longer than the actual length of the pipe. Furthermore, $\tilde{f} = 0.97 \pm 0.02$ has the same order of magnitude as Ito (1970) found for motion on real geophysical scale ($f \approx 1.5$). Hence our experiments give validation to his numerical/empirical value.

Although the use of effective instead of physical pipe length amounts to adjusting the theoretical curves to the measurements, note that only one fit is used for all three curves. For a (hypothetical) linear system there would be no dependence of the response curve on the forcing amplitude. Instead the experiments

show that the height and sharpness of the resonance peak decrease for increasing amplitudes, due to the fact that effective friction r increases, as was already noted qualitatively by Bowers (1977), De Girolamo (1996) and Martinez and Naverac (1988). This decrease of the resonator's quality (resonance frequency divided by peak width) is captured well by Lorentz' linearization theory. The curves for different forcing amplitude are similar to those for different opening width, in which case the effective friction is increased due to an increase of v_0 in our terminology (c.f. Martinez and Naverac, 1988, Fig. 6). Note that quadratic friction not only causes the response curves to be different for different forcing amplitudes but also changes the shape of the curves, because the effective linear friction coefficient $r \sim \omega\alpha$ is not constant along the individual curves either. Although this effect is hardly visible at first sight it causes the curves to drop off slightly steeper to the right of the peak frequency. A conspicuous feature of the phase lag curves is the fact that the phase lag is $-\pi/2$ for $\omega = \omega_0$ irrespective of forcing amplitude. It is immediately clear from (2) that this is predicted by the theory as well.

5. Domain of validity

The correspondence between theory and measurements in Fig. 4 is very good. In the present laboratory setup, conditions for which Lorentz' linearization theory does not perform well have not been found. In order to investigate the domain of validity of Lorentz' linearization theory, model (1) has been studied in more detail, both analytically and numerically.

First of all, it is worthwhile to note that the variables in (1) can be rescaled to obtain a more simple dimensionless model by scaling

$$\zeta = \frac{OL}{A\tilde{f}}\zeta', \quad \zeta_e = \frac{OL}{A\tilde{f}}\zeta'_e, \quad u = \omega_0\frac{L}{\tilde{f}}u', \quad t = \frac{t'}{\omega_0}, \tag{5}$$

which leads to the dimensionless model

$$\frac{du'}{dt'} = \zeta'_e - \zeta' - |u'|u', \tag{6a}$$

$$\frac{d\zeta'}{dt'} = u'. \tag{6b}$$

The only parameters that still determine the behavior of this system are those that determine the forcing water-level elevation ζ'_e at sea, the (dimensionless) forcing frequency $\omega' = \omega/\omega_0$ and amplitude $\alpha'_e = (A\tilde{f}/OL)\alpha_e$. Hence the shape of the response curves is completely determined by the dimensionless parameter α'_e that measures the relative importance of friction.

5.1. First-order corrections to Lorentz' linearization theory

Zimmerman (1992) showed that Lorentz' linearization procedure can be considered as a renormalization method. Introducing a formal expansion parameter ε, (6a) is replaced by

$$\frac{du'}{dt'} = \zeta'_e - \zeta' - \varepsilon|u'|u' - r'u', \tag{7}$$

which equals (6a) for $\varepsilon=1$, $r'=0$. Writing $\zeta'=\bar{\zeta}'+\varepsilon z'+\mathcal{O}(\varepsilon^2)$, $u'=\bar{u}'+\varepsilon v'+\mathcal{O}(\varepsilon^2)$, $r'=\bar{r}'+\varepsilon\rho'+\mathcal{O}(\varepsilon^2)$ and consistently collecting terms of the same order in ε one finds the model with linearized friction to first order. At the next order one has

$$\frac{\mathrm{d}v'}{\mathrm{d}t'}+\bar{r}'v'+z'=-|\bar{u}'|\bar{u}'-\rho'\bar{u}', \tag{8a}$$

$$\frac{\mathrm{d}z'}{\mathrm{d}t'}=v'. \tag{8b}$$

Truncating at this order, the consistency condition $r'=0$ for $\varepsilon=1$ implies that $\rho'=-\bar{r}'$. The renormalization condition, requiring the first-order solution $\bar{\zeta}'$, $\bar{u}'$ to correctly capture the behavior at the forcing frequency ω', consequently leads to $\bar{r}'=(8/3\pi)\omega'|\bar{\alpha}'|$, where $\bar{\zeta}'=\mathrm{Re}[\bar{\alpha}'\,\mathrm{e}^{\mathrm{i}\omega' t'}]$, $\bar{u}'=\mathrm{Re}[\mathrm{i}\omega'\bar{\alpha}'\,\mathrm{e}^{\mathrm{i}\omega' t'}]$ is the Lorentz' linearized solution (to be found from (3) with $v_0=8/3\pi$). This is consistent with Lorentz' energy principle. For the correction z' on the Lorentz' linearized results we thus have (writing $\bar{\alpha}'=|\bar{\alpha}'|\,\mathrm{e}^{\mathrm{i}\bar{\varphi}'}$)

$$\begin{aligned}\frac{\mathrm{d}^2z'}{\mathrm{d}t'^2}+\bar{r}'\frac{\mathrm{d}z'}{\mathrm{d}t'}+z'&=\bar{r}'\bar{u}'-|\bar{u}'|\bar{u}'\\&=-\frac{8}{3\pi}\omega'^2|\bar{\alpha}'|^2\,\sin(\omega' t'+\bar{\varphi}')\pm\omega'^2|\bar{\alpha}'|^2\sin^2(\omega' t'+\bar{\varphi}'),\end{aligned} \tag{9}$$

with the plus-sign if $\sin(\omega' t'+\bar{\varphi}')$ is positive and the minus-sign if it is negative, hence on the intervals, indexed by integer k, $[k(2\pi/\omega')-(\bar{\varphi}'/\omega'),(k+\frac{1}{2})(2\pi/\omega')-(\bar{\varphi}'/\omega')]$ or $[(k+\frac{1}{2})(2\pi/\omega')-(\bar{\varphi}'/\omega'),(k+1)(2\pi/\omega')-(\bar{\varphi}'/\omega')]$. Up to this point the procedure from Zimmerman (1992) was followed, but he solved (9) using a truncated Fourier sum whereas matching exact solutions on the latter intervals is performed here. The solution on the respective intervals is given by

$$\begin{aligned}z'^{(k)}_{\pm}&=\frac{|\bar{\alpha}'|}{1+\delta_1^2}\left(\cos(\omega' t'+\bar{\varphi}')-\delta_1\sin(\omega' t'+\bar{\varphi}')\right)\\&\pm\frac{1}{2}\omega'^2|\bar{\alpha}'|^2\mp\frac{3\pi}{32}\frac{|\bar{\alpha}'|}{1+\delta_2^2}\left(\delta_2\cos(2\omega' t'+2\bar{\varphi}')+\sin(2\omega' t'+2\bar{\varphi}')\right)\\&+B^{(k)}_{\pm}\mathrm{e}^{-(\bar{r}'/2)(t'-t^{(k)}_{\pm})}\cos\left(\sqrt{1-\left(\frac{\bar{r}'}{2}\right)^2}\,(t'-t^{(k)}_{\pm})\right)\\&+D^{(k)}_{\pm}\mathrm{e}^{-(\bar{r}'/2)(t'-t^{(k)}_{\pm})}\sin\left(\sqrt{1-\left(\frac{\bar{r}'}{2}\right)^2}\,(t'-t^{(k)}_{\pm})\right),\end{aligned} \tag{10}$$

where we abbreviate $\delta_1=(3\pi/8)(1-\omega'^2)/(\omega'^2|\bar{\alpha}'|)$, $\delta_2=(3\pi/16)(1-4\omega'^2)/(\omega'^2|\bar{\alpha}'|)$, $\bar{r}'=(8/3\pi)\omega'|\bar{\alpha}'|$ and $t^{(k)}_{+}=k(2\pi/\omega')-(\bar{\varphi}'/\omega')$, $t^{(k)}_{-}=(k+\frac{1}{2})(2\pi/\omega')-(\bar{\varphi}'/\omega')$ are the points at which $\sin(\omega' t'+\bar{\varphi}')$ changes sign. By matching z' and $\mathrm{d}z'/\mathrm{d}t'$ at $t^{(k)}_{\pm}$, we can relate the integration constants $B^{(k)}_{\pm}$, $D^{(k)}_{\pm}$ in subsequent intervals:

$$\mathbf{F}X^{(k)}_{-}=\mathrm{e}^{-(4/3)|\bar{\alpha}'|}\,\mathbf{F}\,\mathbf{R}X^{(k)}_{+}+d\quad\text{and} \tag{11a}$$

$$\mathbf{F}X_+^{(k+1)} = \mathrm{e}^{-(4/3)|\bar{\alpha}'|}\,\mathbf{F}\,\mathbf{R}X_-^{(k)} - d \quad \text{hence} \tag{11b}$$

$$X_+^{(k+1)} = \delta^2\,\mathbf{R}^2 X_+^{(k)} + \delta\,\mathbf{R}\,\mathbf{F}^{-1}d - \mathbf{F}^{-1}d, \tag{11c}$$

in which $X_\pm^{(k)} = \begin{pmatrix} B_\pm^{(k)} \\ D_\pm^{(k)} \end{pmatrix}$ is the vector containing the integration constants,

$$\mathbf{F} = \begin{pmatrix} 1 & 0 \\ -\dfrac{\bar{r}'}{2} & \sqrt{1-\left(\dfrac{\bar{r}'}{2}\right)^2} \end{pmatrix}$$

is a skew matrix incorporating phase differences between currents and water level due to friction,

$$\mathbf{R} = \begin{pmatrix} \cos\left(\dfrac{\pi}{\omega'}\sqrt{1-\left(\dfrac{\bar{r}'}{2}\right)^2}\right) & \sin\left(\dfrac{\pi}{\omega'}\sqrt{1-\left(\dfrac{\bar{r}'}{2}\right)^2}\right) \\ -\sin\left(\dfrac{\pi}{\omega'}\sqrt{1-\left(\dfrac{\bar{r}'}{2}\right)^2}\right) & \cos\left(\dfrac{\pi}{\omega'}\sqrt{1-\left(\dfrac{\bar{r}'}{2}\right)^2}\right) \end{pmatrix}$$

is the rotation matrix over angle $(\pi/\omega')\sqrt{1-(\bar{r}'/2)^2}$ related to the eigenoscillation, the factor $\delta{=}\mathrm{e}^{-(4/3)|\bar{\alpha}'|}$ accounts for frictional damping of the oscillation and

$$d = \begin{pmatrix} \dfrac{9\pi^2}{64(1+\delta_2^2)}(4\omega'^2 + \bar{r'}^2 - 1) \\ \dfrac{-3\pi\omega'|\bar{\alpha}'|}{8(1+\delta_2^2)} \end{pmatrix}$$

is the vector representing the forcing at this order. The stationary solution (independent of k) to these equations is found by solving $[\mathbf{I} - \delta^2\mathbf{R}^2]X_+ = -[\mathbf{I} - \delta\mathbf{R}]\mathbf{F}^{-1}d$, hence $X_+ = -[\mathbf{I} + \delta\mathbf{R}]^{-1}\mathbf{F}^{-1}d$. The complete expression for the sealevel and current oscillation up to this order is obtained by adding $\zeta'_\pm = \bar{\zeta}' + \varepsilon z'_\pm$, $u'_\pm = \bar{u}' + \varepsilon v'_\pm$, setting $\varepsilon = 1$.

Performing an harmonic analysis, fitting a sum of sinusoids with frequencies $n\omega'$, with $n = 0, 1, 2, \ldots$ to ζ', the correction has no influence on the harmonic fit at the forcing frequency, due to the renormalization condition. So the response curves found using Lorentz' linearization procedure need not be changed to this order of approximation. Still, one can use the results from this section to estimate the changes in the tidal curve due to the nonlinear friction term, see Fig. 6.

5.2. Numerical results

The dimensionless model (6) has been integrated using the numerical dynamical systems package DsTool (Guckenheimer et al., 1992) for several values of α'_e between 0.1 and 30. They were subsequently processed in the same manner as the experimental results. In line with the observation at the end of the previous section the response curves are not noticeably different from the prediction by Lorentz'

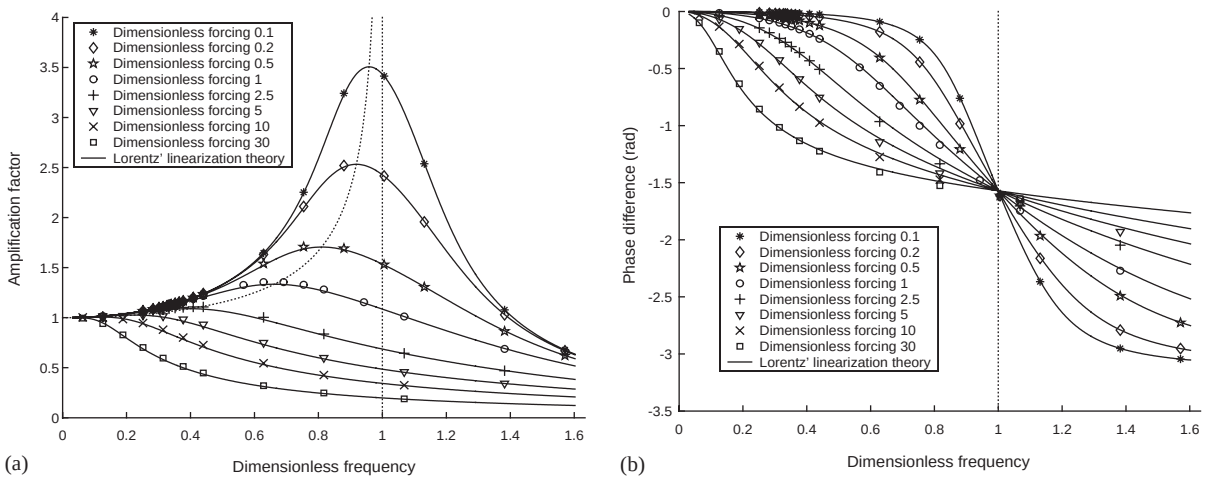

Fig. 5. Response curves: (a) amplification factor and (b) phase lag between the tide at sea and in the basin as a function of forcing frequency. Numerical results (symbols) for the dimensionless system (6) are shown. The dimensionless Helmholtz frequency $\omega'_0 = 1$ is indicated by a dotted vertical line, a dotted curve connects the maxima according to (4). The theoretical (solid) curves are calculated from (3),(4), with $\omega_0 = 1$, $\nu_0 = 8/3\pi$.

linearization theory over this entire range, see Fig. 5. Deviations from Lorentz' linearization theory appear when considering the tidal curves. Fig. 6(a) shows the tidal curve for one of the numerical runs for which the correspondence between the numerical integration of (6) and the theoretical calculations using (10) is the worst, with $\alpha'_e = 2.5$, $\omega' = 0.377$. One can see that the deviations from a single sinusoid are still predicted quite well by the asymptotic correction (10). Note that the current (which has not been measured during the laboratory experiments) is influenced more strongly by the quadratic nature of friction than the water level itself. Subtracting the single sinusoid at the forcing frequency one is left with the deviation from Lorentz' theory in Fig. 6(b), in which it is more clear that correction (10) overestimates the amplitude of the tertiary overtide. This can be seen as well in Fig. 6(c), which shows the maximum deviation relative to the amplitude of Lorentz' sinusoidal response as a function of the forcing frequency for $\alpha'_e = 0.1$, 1 and 30 (asterisks, pluses and crosses). Moreover, it shows the relative change of the high water level (open circles, squares and diamonds), which is less than the maximum deviation because the latter need not be synchronized with high tide. The maximum deviation and the deviation of the maxima according to the asymptotic correction (10) is plotted as well, by dashed and dotted curves, respectively. Actually, we find peaks of resonant behavior at forcing frequencies $\omega' = 1/n$, with n odd, $n = 3$ in particular. The amplitude of the peak is overestimated however, because up to this order of approximation the effective friction coefficient $\tilde{r}' = (8/3\pi)\omega'|\tilde{\alpha}'|$ is normalized for the dominant (forcing) frequency only. The resonant motion at the eigenfrequency is damped more strongly because its frequency is three times the forcing frequency in this case. The main conclusion to be drawn from this figure though, is the fact that Lorentz' theory is correct within 7% even for $\alpha'_e = 30$, for which the response curve Fig. 5 shows damping for almost all frequencies.

5.3. Geophysical context

When extending the model result (3) from the laboratory setting to the geophysical context, the main lack of knowledge is in the relative strength of friction. In the laboratory setting, the dominant dissipative

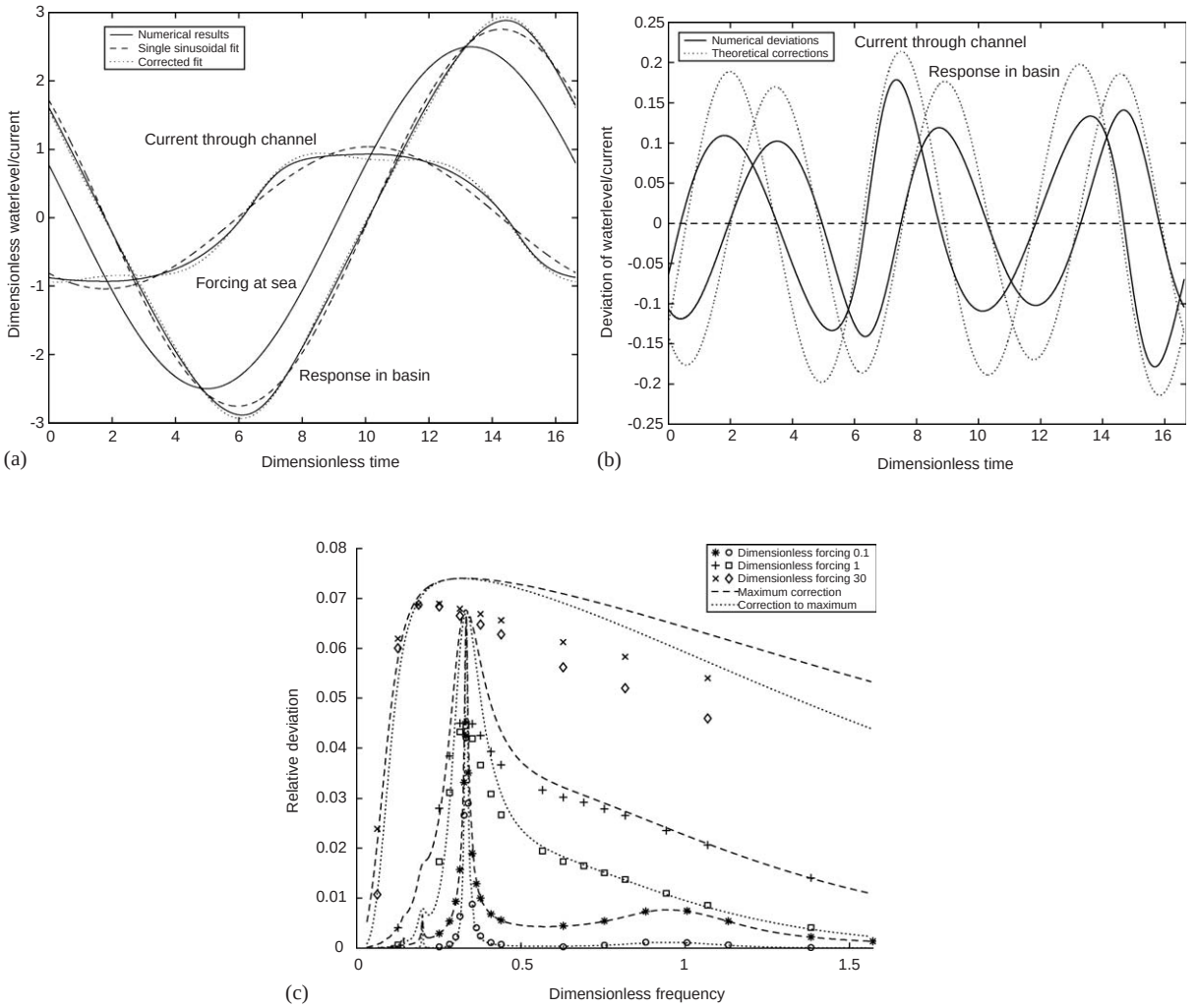

Fig. 6. Numerical results integrating (6) versus theoretical corrections using (10): (a) shows a sample tidal curve for $\alpha'_e = 2.5$, $\omega' = 0.377$. In (b) the dominant signal at the forcing frequency is subtracted. The maximum deviation from this signal (the maximum of the basin's water-level response in (b), asterisks, pluses and crosses) is plotted as a function of forcing frequency ω' in (c), as well as the deviation of the maxima (high tide in (a), circles, squares and diamonds) from the single sinusoid's amplitude predicted by Lorentz' linearization theory, both relative to the amplitude of the single sinusoid. Results are obtained by numerical integration using DsTool for $\alpha'_e = 0.1$, 1 and 30. The dashed lines approximate the maximum deviation, the dotted ones the deviation of the maxima, according to (10). The peak at $\omega' = \frac{1}{3}$ is predicted well, although the amplitude is overestimated.

effect is the head loss due to the constriction. This clearly depends on the shape of the entrance. Although the quadratic dependence of friction on the velocity should still be valid, the appropriate value of the coefficient $\tilde{f}$ is somewhat uncertain. However, because the value $\tilde{f} = 0.97$ found by our laboratory experiments compares well with Ito's (1970) numerical value $f = 1.5$, one is inclined to use this value in the geophysical context as well. For example, the Amelander Inlet in the Dutch Wadden Sea can be

considered to be a Helmholtz basin with the following (approximative) characteristics:

$$A = 2.5 \times 10^8\ \mathrm{m}^2, \quad B = 3 \times 10^3\ \mathrm{m}, \quad H = 10\ \mathrm{m}, \quad L_{\mathrm{eff}} = 5 \times 10^3\ \mathrm{m}, \quad \alpha_{\mathrm{e}} = 1\ \mathrm{m},$$

which leads to

$$\omega_0 = 4.9 \times 10^{-4}\ \mathrm{rad\,s}^{-1}, \quad \omega'_{M_2} = 0.29, \quad \alpha'_{\mathrm{e}} = 1.62 \quad \text{hence } \frac{|\alpha|}{\alpha_{\mathrm{e}}} = 1.082.$$

This compares reasonably well with the observed tide with range 1.4–2.5 m at sea and 1.7–2.8 m on the mainland at neap and spring tide, respectively. Abusively extending the results for a Helmholtz basin to a quarter wavelength resonator, the famous Bay of Fundy leads to surprisingly comparable results as well. Considering only the Bay of Fundy by itself, it has a total length of 270×10^3 m and an average width of about 50×10^3 m leading to $A = 1.35 \times 10^{10}$ m^2. The entrance, 80×10^3 m wide, on average 50 m deep, is estimated with cross-section $O = 4 \times 10^6$ m^2. For the effective length of the entrance we take $L_{\mathrm{eff}} = 100 \times 10^3$ m. Actually, the effective "channel" length for which the Helmholtz frequency corresponds with the first quarter wavelength mode, is found by dividing the total basin length by $\pi^2/4$. The tidal amplitude at the mouth of the Bay of Fundy is 3 m, hence we find, $\omega_0 = 1.7 \times 10^{-4}$ rad s^{-1}, $\omega'_{M_2} = 0.82$, $\alpha'_{\mathrm{e}} = 0.098$ and $|\alpha|/\alpha_{\mathrm{e}} = 2.8$, which compares well with the amplification up to 8 m amplitude within the Bay of Fundy.

6. Conclusion

Although the theoretical foundations of Lorentz' linearization method were already put forward in Lorentz (1922, 1926), no quantitative high-accuracy experimental validation is found in literature yet. The theory has been developed further (Mei, 1989; Kabbaj and Le Provost, 1980; Zimmerman, 1992), comparison with observations have been made (Ito, 1970; Thijsse, 1972), but studies using laboratory experiments have been restricted to validating linear theory mainly (McNown, 1952; Raichlen and Ippen, 1965; Lee, 1971). Experimental papers in which the effect of nonlinear friction on the response curves has been measured, did not provide an explicit quantitative comparison with theory, mainly because the focus was on another topic (Horikawa and Nishimura, 1970; Bowers, 1977; De Girolamo, 1996; Martinez and Naverac, 1988). The experiments discussed in the present paper give a clear validation of Lorentz' linearization principle to describe the influence of quadratic friction on the response curves for the Helmholtz mode in an almost-enclosed basin. A good fit between theory and experiment was found. In particular the observed decrease of the resonator's quality with increasing amplitude corresponds perfectly with the theoretical increase of the effective friction coefficient.

Further research will be focused on improving the quality of the resonator and measuring nonlinear effects from non-uniform hypsometry (Maas, 1997) or continuity/advection (Miles, 1981). The first goal may be achieved by smoothing the pipe ends in order to reduce flow separation or decreasing the basin area, hence the tidal prism. For the second goal, artificial topography can be introduced into the basin mimicking intertidal flats causing the basin area to depend on the water level. According to the theory this may lead to bending of the response curve, multiple equilibria and chaotic behavior of tidal amplitudes, possibly explaining observational reports of drifting harmonic "constants" and chaotic tidal records (Maas and Doelman, 2002, and references therein).

Acknowledgements

We would like to thank Edwin Keijzer, Theo Kuip, Martin Laan and Sven Ober for their support in designing and constructing the experimental setup, and Huib de Swart, Jeff Zimmerman and Arjen Doelman for discussing the manuscript.

References

Aubrey, D.G., Speer, P.E., 1985. A study of non-linear tidal propagation in shallow inlet/estuarine systems. Part I: observations. Estuarine, Coastal Shelf Sci. 21, 185–205.

Bowers, E.C., 1977. Harbour resonance due to set-down beneath wave groups. J. Fluid Mech. 79 (1), 71–92.

Carrier, G.F., Shaw, R.P., Miyata, M., 1971. Channel effects in harbor resonance. J. Eng. Mech. Div. 1703–1716 (Proceedings of the American Society of Civil Engineers).

Defant, A., 1961. Physical Oceanography, vol. 2. Pergamon, Oxford, London, New York, Paris.

De Girolamo, P., 1996. An experiment on harbour resonance induced by incident regular waves and irregular short waves. Coastal Eng. 27, 47–66.

Guckenheimer, J., Back, A., Myers, M., Wicklin, F., Worfolk, P., 1992. dstool: computer assisted exploration of dynamical systems. Notices Am. Math. Soc. 39, 303–309.

Horikawa, K., Nishimura, H., 1970. On the function of tsunami breakwaters. Coastal Eng. J. 13, 103–112.

Ito, Y., 1970. Head loss at tsunami-breakwater opening. In: Proceedings of the 12th ASCE Conference on Coastal Engineering, pp. 2123–2131.

Kabbaj, A., Le Provost, C., 1980. Nonlinear tidal waves in channels: a perturbation method adapted to the importance of quadratic bottom friction. Tellus 32, 143–163.

Lee, J.-J., 1971. Wave-induced oscillations in harbours of arbitrary geometry. J. Fluid Mech. 45, 375–394.

Lepelletier, T.G., Raichlen, F., 1987. Harbor oscillations induced by nonlinear transient long waves. J. Waterway, Port, Coastal Ocean Eng. 113 (4), 381–400.

Lorentz, H.A., 1922. Het in rekening brengen van den weerstand bij schommelende vloeistofbewegingen. De Ingenieur, p. 695 (in Dutch).

Lorentz, H.A., 1926. Verslag Staatscommissie Zuiderzee 1918–1926. Alg. Landsdrukkerij, Den Haag (in Dutch, report senate committee Zuiderzee).

Maas, L.R.M., 1997. On the nonlinear Helmholtz response of almost-enclosed tidal basins with sloping bottoms. J. Fluid Mech. 349, 361–380.

Maas, L.R.M., Doelman, A., 2002. Chaotic tides. J. Phys. Oceanogr. 32 (3), 870–890.

Martinez, F.M., Naverac, V.S., 1988. An experimental study of harbour resonance phenomena. In: Edge, B.L. (Ed.), Proceedings of the 21st International Conference on Coastal Engineering, ASCE, Torremolinos, pp. 270–280.

McNown, J.S., 1952. Waves and seiche in idealized ports. In: Gravity Wave Symposium, Number 521 in National Bureau of Standards Circular, pp. 153–164.

Mei, C.C., 1989. The Applied Dynamics of Ocean Surface Waves. World Scientific, Singapore.

Mei, C.C., Liu, P.L.-F., Ippen, A.T., 1974. Quadratic loss and scattering of long waves. J. Waterways, Harbors Coastal Eng. Div. 100, 217–239.

Miles, J.W., 1974. Harbor seiching. Annu. Rev. Fluid Mech. 6, 17–35.

Miles, J.W., 1981. Nonlinear Helmholtz oscillations in harbours and coupled basins. J. Fluid Mech. 104, 407–418.

Parker, B.B., 1991. The relative importance of the various nonlinear mechanisms in a wide range of tidal interactions(review). In: Parker, B.B. (Ed.), Tidal Hydrodynamics. Wiley, New York, pp. 237–268.

Raichlen, F., Ippen, A.T., 1965. Wave induced oscillations in harbors. J. Hydraul. Div. 1–26 (Proceedings of the American Society of Civil Engineers).

Thijsse, J.T., 1972. Een halve eeuw Zuiderzeewerken. Tjeenk Willink, Groningen (in Dutch).

Zimmerman, J.T.F., 1992. On the Lorentz-linearization of a nonlinearly damped tidal Helmholtz oscillator. Proc. KNAW 95 (1), 127–145.